Microfluidic Investigation Reveals Distinct Roles for Actin Cytoskeleton and Myosin II Activity in Capillary Leukocyte Trafficking

Sylvain Gabriele, Anne-Marie Benoliel, Pierre Bongrand, Olivier Théodoly

Microfluidic investigation reveals distinct roles for actin cytoskeleton and myosin II activity in capillary leukocyte trafficking

Sylvain Gabriele[1,*], Anne-Marie Benoliel[1], Pierre Bongrand[1] and Olivier Théodoly[1]

[1]Université de la Méditerranée, Adhésion & Inflammation, INSERM U600-CNRS UMR6212, Case 937, 163 Avenue de Luminy, F-13009 Marseille, France

*Present address : Université de Mons-Hainaut, Interfaces & Fluides Complexes, 20, Place du Parc, B-7000 Mons, Belgique

Summary

Circulating leukocyte sequestration in pulmonary capillaries is arguably the initiating event of lung injury in Acute Respiratory Distress Syndrome (ARDS). We present a microfluidic investigation of the roles of actin organization and myosin II activity during the different stages of leukocyte trafficking through narrow capillaries (entry, transit and shape relaxation) using specific drugs (Latrunculin A, Jasplakinolide and Blebbistatin). The deformation rate during entry reveals that cell stiffness depends strongly on F-actin organization and hardly on myosin II activity, supporting microfilament role in leukocyte sequestration. In the transit stage, cell friction is influenced by stiffness, demonstating that the actin network is not completely broken after a forced entry into a capillary. Conversely, membrane unfolding was independent of leukocyte stiffness. The surface area of sequestered leukocytes increased by up to 160% in absence of myosin II activity, showing the major role of molecular motors on microvillus wrinkling and zipping. Finally, cell shape relaxation was largely independent of both actin organization and myosin II activity, whereas a deformed state was required for normal trafficking through capillary segments.

Introduction

The mechanical plugging of lung microvessels by leukocytes has been implicated in the pathophysiology of several diseases, e.g. Acute Lung Injury (ALI). The estimated 190,000 cases of ALI in the United States generate high expenses, and the Acute Respiratory Distress Syndrome (ARDS), the most hypoxemic ALI presentation, results in a mortality rate ranging from 34 to 58% (Frutos-Vivar et al., 2004; MacCallum and Evans, 2005). ARDS is a challenging entity for clinical investigation because it lacks an accepted diagnostic test and relies on a panel of clinical findings for diagnosis. Leukocyte sequestration has been reported after sepsis, trauma, hemorrhagic shock or ischemia (Schmid-Schönbein, 1987; Hansell et al., 1993) and sequestration in lung microvasculature is considered as the initiating event in the development of ARDS (Worthen, 1989; Thiel, 1996).

Studying mechanisms of leukocyte sequestration (adhesion and/or low deformability) in humans is difficult. Recent evidence demonstrated that initial stages of neutrophil sequestration in rats are not due to CD11-CD18 mediated adhesion, supporting a major involvement of leukocyte mechanical properties in sequestration (Yoshida et al., 2006). Also, leukocyte mechanical behavior was investigated with many techniques aimed at quantifying leukocytes deformability and rheology under various conditions, including centrifugation (Fukuda and Schmid-Schönbein, 2002), cell poker (Petersen et al., 1982), polycarbonate filter (Franck, 1990), parallel plates (Thoumine and Ott, 1997), atomic force microscopy (Rotsch and Radmacher, 2000), optical tweezers (Sheetz, 1998), microrheometry and micropipette aspiration (Chien et al., 1987, Richelme et al., 2000; Drury and Dembo, 1999). Despite considerable efforts, no universal rheological model could be obtained and the precise role of the three major filamentous constituents of the cytoskeleton, microtubules (Chien et al., 1987; Tsai et al., 1998), intermediate filaments (Brown et al., 2001) and actin filaments (Sheikh et al., 1997), in leukocyte mechanical properties remains poorly understood.

Actin filaments previously appeared as a primary structural determinant of neutrophil mechanical properties (Sheikh et al., 1997; Tsai et al., 1998). Furthermore, Nishino and coworkers demonstrated that neutrophils from septic shock and ARDS patients were significantly more rigid than controls and observed a change of actin network polymerization (Nishino et al., 2005). Evidence for the formation of an actin-rich rim in the submembrane region of deformed (Yap and Kamm, 2005) and ARDS patient (Nishino et al., 2005) leukocytes raises questions regarding the precise role of actin microfilament organization in the mechanical changes of circulating leukocytes (Pai et al., 2008). On the other hand, Lämmermann and coworkers recently demonstrated that myosin II-dependent contraction of migrating leukocytes was required on passage through narrow gaps (Lämmermann et al., 2008), suggesting an important contribution of molecular motors in the

behaviour of leukocytes sequestered in narrow capillaries. These results underline the interest of investigating the precise roles of actin and actomyosin activity in capillary leukocyte trafficking.

Significant insight in the rheological properties of model leukocytes in microcapillaries, such as HL60 or THP-1 cells, have been obtained by micropipette aspiration, but only in the first stage of leukocytes entry into constriction. Additional information on the following stages (capillary transit and shape recovery) in physiologically relevant hydrodynamical conditions is needed. Microfluidics versatility allows physiologically relevant testing on the whole passage process (Yap and Kamm, 2005; Chaw et al., 2006) and may be more relevant to clinical problems.

Here, we present an efficient microfluidic approach to measure new relevant parameters of leukocyte transit in narrow capillaries, such as entry time, cell velocity in the constriction, cell morphology during the capillary transit through a constriction, shape recovery kinetics after passage and effect of a first deformation on the passage through following segments. We intend to define the specific role of actin cytoskeleton and actomyosin activity in the passage of circulating leukocytes through narrow capillaries. This issue is addressed by specifically enhancing or inhibiting actin cytoskeleton and actomyosin activity. We used actin-specific agents with well described molecular effects: latrunculin A, LatA, is a potent microfilament inhibitor (Wong et al., 2005), jasplakinolide, Jpk, stabilizes actin filaments (Bubb et al., 1994) and Blebbistatin, Blb, specifically inhibits myosin II activity in leukocytes (Straight et al., 2003). We confirm the major role of actin filaments organization on the deformation rate during the entry stage. Our results also bring new insights into the specific role of actin cytoskeleton and myosin II activity during the transit stage of a leukocyte in a constriction. We show that the cell velocity in the constriction is lower as the actin network is more organized and that the sequestered cell morphology is controlled by myosin II activity. For the last stage after release from a constriction, we found that actin organization and molecular motor activity did not influence the shape recovery process and that a deformed state plays an important role for normal trafficking through successive capillary segments.

Results

Microfluidic experiments

The microfluidic device (Fig. 1A) we used is composed of an inlet channel, a 4-μm-wide constriction channel and a relaxation channel. A typical experiment consists of recording the different stages of a single cell crossing the 4-μm-wide constriction, i.e. entry, transit, and shape recovery after release (supplementary material Movie 1). The constraint applied to the cells corresponds to physiological flow conditions maintained by applying constant hydrostatic pressure across the constriction. A calibration was performed by tracking fluorescent micron-size particles in the constriction to measure the maximum fluid velocity, MxFV, against the applied pressure (Fig. 1B).

Cell entry times are dependent on actin cytoskeleton organization

Leukocyte deformability was assessed by measuring the time required for the cells to completely enter the constriction. Fig. 2 shows a typical sequence of the large deformation displayed by a THP-1 cell entering the narrow capillary. We defined the entry time (ET), as the time interval between the leading edge of the cell crossing the entry into the microchannel and its trailing edge clearing the entry. Serial single-cell entry time measurements as a function of applied driving pressures (Fig. 3A) were taken 30 minutes after exposure to Jpk (3 μM) and LatA (3 μM). Generally, the ET decreases with driving pressure and the dependency of ET on cell treatments is enhanced at low driving pressures. In the presence of Jpk, THP-1 cells exhibited very long ETs of more than 700 seconds at low driving pressure (6 cm H_2O), approximately threefold higher than controls. Conversely, the average ET of LatA-treated cells was approximately 2 times lower than ET of controls at low driving pressure. Further, ET observed on Blb-treated cells exhibited only minor differences with controls. Thus, the ETs of THP-1 cells in a narrow capillary are mainly affected by the passive actin cytoskeleton organization and marginally by molecular motor activity.

Cytoskeletal organization influences cell deformation kinetics

By plotting the length of the cell projection in the constriction, L_p, versus time, t, we analyzed the dynamics of deformation of control and treated THP-1 cells. As shown in Fig 3B for low pressure drop (10,8 cm H_2O), the kinetics of cell entry appeared as a sigmoid with three phases. First, cytoplasm flew rapidly into the microchannel. Then, at the middle phase, cell entry rate decreased and approached a quasi-steady regime as the cell crept into the microchannel with a nearly constant velocity. Finally, in the third phase, the cell flow was

dramatically accelerated as the last part of the cell entered the microchannel. The width of the steady stage was largest for Jpk-treated cells and shortest for Lat-treated THP-1 cells. Therefore, projection length dynamics indicate that the deformation rate is strongly dependent on the actin network, especially in the quasi-steady regime. Blb-treated cells displayed weakly increased deformability, suggesting that myosin II activity retards leukocyte deformation by slightly increasing mechanical resistance.

The actin cytoskeleton organization controls cell velocity in the constriction by friction force modulation

Our microfluidics setup allowed us to study cell transit in a long constricted capillary. The cell velocity was observed to be constant all along the 2250 μm long constriction, therefore the mean cell velocity, MnCV, was determined using the time interval between the trailing edge of the cell clearing the entry and its leading edge clearing the constriction. The maximum fluid velocity, MxFV, was experimentally obtained for each driving pressure by tracking fluorescent beads in the absence of cells in the constriction and the corresponding mean fluid velocity, MnFV, was calculated according to the velocity profile in rectangular microchannels (Tabeling, 2005). Fig 4A shows the evolution of MnCV/MnFV ratios as a function of the applied driving pressure. A MnCV/MnFV ratio close to one means that the friction force, F_f, due to retarding Couette flow-induced shear stress between the cell and the wall, are negligeable compared to the the pressure-drop-induced force, F_p. Conversely, a MnCV/MnFV ratio close to 0 corresponds to conditions where F_f is large as compared to F_p. Two clear trends can be observed in Fig. 4A. First, the MnCV/MnFV ratios tend to one for control and treated-cells at the highest driving pressures (above 30 cm H_2O), meaning that F_f is negligeable compared to F_p. On the other hand, one can see that the MnCV/MnFV ratios at low driving pressures decrease to values significantly smaller than one for control and treated cells. Therefore, our microfluidic setup allows us to gain insight into the resistance to cell transit in the capillary, provided surface structures are comparable. Disruption of actin organization (with LatA) is characterized by a high MnCV/MnFV ratio (~ 0.7) at the lowest applied driving pressure, as compared to control cells (MnCV/MnFV ratio ~ 0.35), whereas a stabilization of the actin network (with Jpk) leads to a very low MnCV/MnFV ratio (~ 0.1). On the other hand, the MnCV/MnFV ratios of Blb-treated THP-1 cells were observed to be very similar to control cells for the whole range of pressure drops. These results demonstrate that friction between circulating leukocytes and capillary walls is hardly influenced by myosin activity and strongly dependent on actin cytoskeleton organization.

Myosin II activity controls the sequestered cell membrane unfolding

To provide further insight into the sequestered cell morphology, we examined the differences of the maximum axial length, L_m, along the capillary axis during the cell transit in the constriction. It is important to note that no significant evolution of L_m was observed during the deformed cell transit, suggesting that L_m is only dependent of the cell entry process.

As a morphological reference, we used the diameter of the puck, D_{pu} = 16.8 μm, obtained by squeezing, at constant volume a spherical cell of initial diameter D_i = 12.5 μm between two parallel walls distant of W = 4 μm, which corresponds to the experimental constriction width (see material and methods section). Two different trends can be distinguished on Fig. 4B. A first behaviour corresponds to control, Jpk-treated and Lat-A-treated cells, for which L_m/D_s is always close to one. The second behaviour corresponds to Blb-treated cells, for which L_m/D_s is always higher than 1 and reaches a maximal value of 1.7 at the lowest applied driving pressure. This finding strongly suggests that only Blb-treated cells exceed the minimal deformation of the reference puck of diameter D_{pu} and heigtht W. In order to determine to the exact morphology of confined cells, we need to get access to a side-view of the cell. This side-view can be obtained in the relaxation channel, where released cells rotate freely, allowing access to new angles of sight on the deformed cells (supplementary material Movie 2). A good approximation of the side view of a confined cell was obtained from the image of the released cell corresponding to a maximum area. The delay after release of the side-view pictures (~ 1 seconds) was always short as compared to the shape recovery time (~ 50 seconds), which insures that the cell morphology is still close to its morphology in the constriction. Fig. 4C shows sequences of three microscopic pictures for THP-1 cells taken shortly after release, (i) in the inlet channel (pictures a), (ii) in the constriction channel (pictures b), and (iii) in the streamer channel (pictures c). These images correspond respectively to the undeformed spherical cell, the top-view and the side-view of the sequestered cell. The morphologies observed for normal, Jpk- and LatA-treated cells (Fig. 4C case I) were all similar and correspond exactly to the puck of diameter D_{pu} and width W, i.e. to the minimal geometric deformation required for a sphere to enter our microfluidic constriction. The ratio between the cell surface in its puck shape, S_{pu}, and its initial spherical shape, S_i, can be determined using:

$$S_{pu}/S_i = \frac{D_i}{3W} + \sqrt{\frac{2W}{3D_i}}$$

S_{pu}/S_i is about 1.5, which corresponds to an excess of cell membrane surface of 50% in the deformed state of case I. On the other hand, the image sequence of case II of the Fig. 4C is typical of Blb-treated cell in the constriction at a low applied driving pressure (13,7 cm H_2O). The cell morphology in the constriction corresponds roughly to a parallelepiped with rounded edges of dimensions 4, 16 and 29 μm. The cross-section dimension 4x16 μm of the deformed cell matches the cross-section WxH of the constriction. The ratio between the cell surface in its parallelepipedic shape, S_{pa}, and its initial spherical shape, $S_{i,}$ is expressed as:

$$S_{pa}/S_i = 2\left(\frac{HW + WL_m + HL_m}{\pi D_i^2}\right)$$

S_{pa}/S_i is about 2.6, which corresponds to an excess of cell membrane surface of 160% in the deformed state for the cells of case II in Fig. 4B. These data suggest that inhibition of molecular motors induces a large cell membrane increase at low applied pressures as compared to the minimal surface increase required to enter the constriction.

Actin organization and actomyosin activity do not influence the shape recovery process

After crossing the 4-μm-wide constriction, the cells were released in a 20-μm-wide channel, which allowed us to observe the shape relaxation, free of external constraints (Fig. 5). The kinetics of shape recovery was studied quantitatively by monitoring the long-to-short axis ratio, l/s, (insert of the Fig. 6). Since the cell can rotate in the relaxation channel, one has to take care of selecting the picture corresponding to the same sight of view. The temporal evolution of the l/s ratio is presented on the Fig. 6 for control, Jpk-, LatA- and Blb-treated THP-1 cells. The effect of F-actin stabilization (with Jpk), actin disruption (with LatA) or myosin II activity inhibition (with Blb) did not affect the dynamics of leukocyte shape recovery, as compared to the unstimulated control groups (THP-1). Furthermore, the shape relaxation kinetics could be divided into two distinct regimes. The first regime is characterized by a fast relaxation of the long-to-short axis ratio down to around 1.3. At the end of this regime, the deformed cell shape corresponds to the image of Fig 5d. This relaxation process took approximatively 50 seconds for control, Jpk-, LatA- and Blb-treated THP-1 cells (Fig. 6). The second regime allows total recovery of the initial spherical shape and takes several hundreds of seconds.

Leukocyte maintained deformed shape facilitates the transit through physiological capillary segments

Physiologically, leukocytes traverse between 50 and 100 segments, in a single passage through the extensively interconnected pulmonary microcirculation (Hogg et al., 1994; Bathe et al., 2002). Compared to the micropipette technique, microfluidic devices allow in-vitro investigations of leukocyte trafficking in channels with more physiologically relevant designs. In a first improvement to approach physiological channel geometries, we changed the long and single constriction channel for a succession of short and narrow segments of width 5 μm and length 20 μm to mimic the capillary segments in the human lungs, which have an average diameter of 5 μm and a length of 11 μm (Weibel, 1963). A typical sequence of leukocyte transit through these successive capillary segments is presented in the Fig. 7 (see also supplementary material Movie 3). We find that the entry time is about 25 seconds in the first constriction and about 0.5 second in all subsequent constrictions. This experiment illustrates that maintaining a deformed shape (l/s ~ 1.5) facilitates the leukocyte transit through the capillary network.

Discussion

In vivo, leukocytes experience a range of different capillary diameters and driving pressures, causing them to stop and undergo large deformations in order to pass through. Increased transit times lead to an accumulation of leukocytes in pulmonary microvessels (Downey and Worthen, 1988; Hogg et al., 1988), which has been implicated in the pathophysiology of a number of diseases. However, the direct study of leukocyte retention in humans is a difficult task. Therefore, several micromanipulation techniques have been proposed to study the mechanical behaviour of non-adherent cells (e.g. leukocytes) in vitro. Important rheological information was obtained by micropipette aspiration, which permits one to mimic the deformation of a leukocyte in the capillary entry stage but is not appropriate to study other stages of the leukocyte passage, such as transit dynamics.

Polycarbonate filter experiments provide a method for quantifying the transit time of leukocyte in narrow pores but do not allow a direct observation of the sequestered cells. None of the conventional techniques have successfully permitted to study the mechanisms (adhesion and/or low deformability) involved in each stage of the leukocyte passage through physiological narrow capillaries. For this purpose, we designed a microfluidic device to study at the single cell level: (i) the entry, (ii) the transit and (iii) the shape relaxation stages of the passage of leukocytes in a constriction. Pulmonary capillaries vary in radius from 1 to 7,5 μm in humans, with a mean of 3,7 μm (Doerschuk et al, 1993). Consequently, we used a 4-μm-wide capillary constriction connected to 20-μm-wide inlet and outlet channels. It was also critical to consider a large range of physiological driving pressures to investigate the leukocyte response to controlled hydrodynamic forces (Huang et al., 2001; West and Mathieu-Costello, 1995). Our microfluidic setup mimics physiological flow conditions, by maintaining a large range of hydrostatic pressures constant over time, which is the best representation of the physiological condition (Hochmuth and Needham, 1990; Huang et al., 2001).

Former studies have shown that actin filaments are a primary structural determinant of leukocyte mechanical properties (Bornens et al. 1989, Sheikh et al., 1997; Tsai et al., 1998). Moreover, recent studies comparing normal and ARDS patient leukocytes demonstrated that leukocytes from sepsis shock and ARDS patients are significantly more rigid than normal leukocytes and exhibit an actin-rich rim in the submembrane region (Skoutelis et al., 2000; Nishino et al., 2005). This strongly suggests a specific role of actin cytoskeleton organization in the sequestration and traffic through microvasculature. On the other hand, the mechanical properties of eukaryotic cells are also dependent on cytoskeletal tension generated by non-muscle myosin II, which apply forces by moving actin filaments relative to each other (Sheetz et al., 1986; Jay et al., 1995; Wakatsuki et al. 2003; Martens and Radmacher, 2008). It was also recently demonstrated that the passage of leukocytes through narrow gaps during transmigration requires squeezing contractions (Lämmermann et al., 2008), and that leukocytes confined in 2D or 3D exhibit myosin driven blebbing motility (Charras and Paluch, 2008). Taken together, these results raise questions regarding the precise role of actin organization and molecular motor activity in the mechanical behaviour of circulating leukocytes during their passage through the lung microvasculature. In the present work, we have tested these hypotheses by studying the role of cytoskeleton organization and/or molecular motors activity in each stage (entry, transit, and shape relaxation) of the passage through microfluidic capillaries, by exposing cells to specific inhibitors of actin polymerization/depolymerisation (LatA and Jpk) and myosin II activity (Blb).

Actin cytoskeleton organization controls entry into capillaries

The sigmoidal curve of the projection length versus the time in the constriction entry stage is consistent with previous investigations of leukocyte deformation with micropipette aspiration (Richelme et al., 2000; Drury and Dembo, 1999). This clearly validates the microfluidic approach as an efficient technique to study the mechanical behaviour of circulating cells. A key observation of cell entry is that leukocytes, which initially show a spherical shape require a finite time to deform in the constriction. The presence of the nucleus may a priori contribute to the relative lack of deformability of leukocytes, especially in the case of our monocytic cell line (THP-1), because the width of our constriction is close to the mean diameter of monocytic nucleus (Schmid-Schonbein et al., 1980). However, the results observed with LatA-treated THP-1 cells demonstrate that leukocytes with disrupted microfilaments enter in the constriction in very short times (Fig. 3A), even at low applied driving forces. This indicates that the mechanical behaviour of leukocytes in our 4-μm-wide constrictions is independent of the viscoelastic nucleus and emphasizes the dominant role of the cytoskeleton. Moreover, our results show that large deformations are facilitated by disruption of actin filament organization and that the retardation of cell transit increases with actin polymerization. This demonstrates that leukocytes must reorganize their actin cytoskeleton to deform into microcapillaries. On the other hand, our data obtained on Blb-treated leukocyte, for which ATPase activity is reduced to 5 % of their initial value (Straight et al., 2003), indicate that a drastic reduction of actomyosin activity reduces only slightly the ET. This observation is consistent with the slight decrease of actin cytoskeleton stiffness reported by Martens and coworkers on myosin II inhibited fibroblasts (Martens et al., 2008). Therefore, the contribution of myosin II for the cell entry stage is certainly weak, as compared to the large importance of actin microfilament organization.

Actin cytoskeleton controls pressure and friction with capillary walls

In previous reports of cell transit through narrow capillaries, the strength of the pressure-drop force F_p pushing the cells through the capillary was always dominating the friction force F_f resulting from hydrodynamic forces between the cell and the capillary walls (Hochmut and Needham, 1990; Bathe et al., 2002; Yap and Kamm, 2005). Our microfluidic devices were designed to access flow conditions where the relative strength of F_f against F_p is high enough to observe deviations of cell velocities from the mean fluid velocity. This has permitted us to investigate the effect on friction of actin organization and actomyosin activity for cells circulating in

constrictions. It is important to recall here that there are no physical contacts between the cells and the walls, so that friction is not due to direct interactions between the cells and the capillary walls. In vivo, the gap between the trafficking cell and the endothelial cells is composed of two layers. Close to the wall, the endothelial glycocalyx layer has a thickness of approximately 500 nm (Vink and Duling, 1996). Between the glycocalyx and the trafficking cell, the lubrication layer contains only medium fluid. The flow of liquid in the glycolcalyx layer was shown to be low as compared to the flow in the lubrication layer (Damiano, 1998). Therefore, the fluid velocity gradient and hydrodynamic shear stress between the cell and the walls in vivo occurs mainly in the lubrication layer. In our experiments with artificial walls, there is a lubrication layer but no endothelial glycocalyx layer. Nevertheless, since friction arises mainly from the hydrodynamic shearing in the lubrication layer, the force F_f is expected to be comparable in vivo and in our microfabricated channels. Only the effects of glycolyx layer compliance under stress (Vink and Duling, 1996) are not taken into accont in our experiments. For a given cell and capillary geometry, the ratio between the friction force F_f and the pressure force F_p depends on the applied driving pressure as:

$$\frac{F_f}{F_p} \propto \frac{v}{\Delta P \delta}$$

where v is the cell velocity, ΔP is the applied pressure and δ is the lubrication film thickness. In conditions where the friction forces are negligible against pressure forces, the velocity v is proportional to ΔP and the lubrication layer thickness δ varies as a power law of velocity with an exponent 2/3 (Bico and Quéré, 2002). The ratio $\frac{F_f}{F_p}$ can then be expressed as:

$$\frac{F_f}{F_p} \propto \frac{1}{v^{2/3}}$$

where the relative importance of friction forces versus pressure forces appears to decrease with velocity. This means that for high driving pressures, friction forces are negligible and the cell velocity is controlled by pressure forces only. This explains why, on Fig. 4A, all MnCV/MnFV ratios tend to 1 at high driving pressures. Conversely, at low applied driving pressures and low cell velocities, the relative effects of friction are enhanced, which explains that we observe various effects of actin cytoskeleton organization and actomyosin activity on friction. For a given channel geometry and applied driving pressure, the main parameter controlling the strength of F_f is the thickness of the lubrication film, δ. A lower cell velocity can be attributed to a thinner lubrication layer between the cell and the walls, and therefore to a higher pressure exerted by the cell on the walls. Using this point of view, several pieces of information can be obtained in the transit stage from the experimental cell velocity differences. First, since different cells exhibit different friction values, it is clear that they do not behave like simple Newtonian liquid drops. The elastic component of the rheological behaviour of leukocytes has to be taken into account in order to understand the differences of transit velocities. Many micropipette investigations have characterized the viscoelastic behaviour of leukocytes on the capillary entry stage (Schmid-Schönbein et al., 1981; Sung et al. 1988), but we present here the first evidence that viscoelastic effects play a significant role in the leukocyte transit through a narrow capillary. Secondly, the fact that Jpk-treated and LatA-treated cells exert respectively higher and lower pressures on the walls as compared to normal cells demonstrates that the cell elastic component exerting a pressure on the walls arises significantly from the actin network organization. Thirdly, velocity results give a direct proof that the rheological state of normal, Jpk- and LatA- treated cells is very different after their entry in the constriction. The forced entry of normal and Jpk-treated cells in narrow constrictions does not completely disrupt their actin scaffold. Fourthly, the instant velocity for all cells was always observed to be constant during the whole cell transit along the capillary. This means that no major change occurs in the cell rheological properties during the transit through the capillary, whatever the friction between the cell and the walls, and despite the large length of the constriction used in this study as compared to physiological constrictions. This supports the observation of Yap and Kamm that the activation of cells (pseudopod formation, increase of F-actin content) by the passage though a constriction occurs for extremely large deformations, in their case for a capillary diameter of 3 μm, i.e. a cross-section of 7 μm^2 (Yap and Kamm, 2005). As a comparison, our constrictions have a cross-section of 64 μm^2. Deformation, more than friction, seems to be an important mechanical trigger of leukocytes activation. On the other hand, we have found that myosin II activity does not influence significantly velocity and friction. Therefore, friction is strongly influenced by actin network organization and hardly by myosin II activity, exactly like stiffness. This supports the idea that stiffness and friction are highly correlated and that the apparent friction is a consequence of cell stiffness.

Membrane unfolding: Myosin II activity contributes to microvily zipping

It is well known that excess leukocyte plasma membrane area is stored in folds and villi, as shown by scanning electron microscopy (Bessis, 1973), and it has been suggested recently that wrinkles are stabilized by membrane-cytoskeleton-membrane bonds (Herant et al., 2003). Plasma membrane wrinkles are a key source of membrane

expansion. During the deformation of a spherical cell, the required increase in membrane area is recruited from this reservoir of membrane by wrinkles smoothing out. This phenomenon is largely involved in the phagocytosis process of leukocytes (Simon and Schmid-Schönbein, 1988). Upon passage through a constriction, a cell undergoes a deformation from its spherical shape that requires membrane unfolding. In our experiments, we have seen that the extension length of leukocytes in the constriction, L_m, does not evolve during the cell travel inside the capillary. The whole deformation process occurs during the entry stage and the exact shape of the deformed cell can be determined at the exit of the constriction from both side and top views.

An interesting feature of our experiments is that normal THP-1 leukocytes exhibit exactly a deformation from a sphere to a puck, which corresponds to the minimal deformation required to enter our constriction. This implies the existence of a mechanism that resists excess membrane unfolding. Herant and coworkers have observed a similar resistance to membrane area expansion against osmotic pressure tending to swell leukocytes (Herant et al., 2003) and they introduced the concept of a « molecular velcro » mechanism holding the wrinkles together. The nature of the molecular velcro remains however largely unknown (Dewitt and Hallet, 2007). Our results also show that Jpk- and LatA- treated cells behave the same way as controls, which demonstrates that alteration of actin filaments does not play a significant role in the resistance to cell membrane unfolding, at least in the range of stresses applied to the cells in our experiments. On the other hand, Blb-treated cells exhibit a large excess unfolding under similar applied stress conditions. The surface increase for Blb-treated cells sequestered in the 4-µm-wide capillary can be as high as 160%, whereas the minimal deformation to enter the constriction is only of 50%. This result clearly demonstrates that the mechanism that resists membrane unfolding, i.e. the molecular velcro mechanism, involves myosin II activity. Moreover, it is remarkable that the membrane area increase of 160% is comparable to the maximum excess area determined experimentally by micropipettes experiments (Evans et al., 1993; Raucher and Sheetz, 1999). This suggests that Blb-treated cells in our experiments have unfolded the totality of their reservoir membrane wrinkles. The wrinkles velcro gripping appears to be very weak with Blb treatment, which raises an important question: does the role of myosin II activity in the velcro gripping mechanism consists of reinforcing the static strength of gripping, or in accelerating the dynamic re-formation of new links and wrinkles? The exact function for most myosins is not completely understood but myosin II activity is always associated with contractile activity, e.g. in cytokinesis (pining apart of a dividing cell) or migration (forward translocation of the body of a cell). The contractile function of myosin II is therefore more consistent with the idea that myosin II participates to membrane wrinkle formation by pulling on actin filaments anchored at different points of the membrane.

Following this point of view, it is interesting to remark that Blb-treated cells do not all exhibit a maximum unfolding. The Blb-treated cells undergoing the highest applied driving pressure and fastest entry process exhibit a minimum membrane unfolding (i.e. membrane surface increase of 50%) exactly like control cells. This result shows that wrinkle grips still exist in Blb-treated leukocytes before application of a mechanical stress/deformation and therefore that myosin II activity is not necessary for the existence of the links. This is consistent with the idea that a Blb treatment inhibits the ATP driven activity of Myosin II but not its binding (and cross-linking) function to actin filaments. Therefore, with Blb treatment, myosin II keeps its passive role of actin filaments molecular cross-linker. Also, it is important to remark that velcro unzipping takes place for the lowest mechanical stress intensity and for the lowest frequencies of the mechanical sollicitation. This proves that the velcro ungripping is not accountable for a decrease of the static gripping strength but rather to a dynamic effect. The ungripping of velcro grips has a finite characteristic detachment time, which is about 50 seconds in our experiments. Consequently, our experiments show also that the characteristic time of wrinkle re-formation is necessarily lower than 50 seconds with Blb treated cells, since we can visualize the cells in their unfolded state. This strongly suggests that myosin II activity is directly involved in the dynamic mechanism of wrinkle re-formation and that this mechanism is not fast enough in Blb-treated cells to compensate the increase of membrane surface. This supports our previous hypothesis that the role of myosin II activity in the membrane folding and wrinkling properties of leukocytes is mainly involved in the dynamics of wrinkle re-formation, most probably by exerting forces between different anchoring points on the membrane (Fig. 8).

Membrane unfolding has not been investigated in diseases implicating leukocyte sequestration in pulmonary capillaries. Indeed, most investigators have focused on the effects of cell mechanical and adhesive properties (Doerschuk, 2001). They have established that the first leukocytes/endothelium contacts are mediated by selectins and their counterreceptors (Kansas, 1996) and that known adhesion molecules, including L-selectin, P-selectin and CD11/CD18, have no role in the initial leukocyte sequestration in the pulmonary microvasculature (Wang et al., 2001; Yoshida et al., 2006). Our microfluidic experiments confirm that cell stiffness is indeed highly correlated to the initial sequestration of leukocytes, and support therefore that adhesion is not required. On the other hand, we also show that the initial leukocyte sequestration implies that cells undergo hydrodynamic elongation forces over long period of times exceeding the characteristic time of membrane velcro unzipping that we determined around 50 seconds. A cell arrest therefore makes possible membrane unfolding. Furthermore, in-vivo inflammation effects can play a role of promoting sequestred cell activation and membrane unfolding. Indeed, the force necessary to ungrip membrane wrinkles is significantly

reduced in activated neutrophils (Herant et al., 2005) and some studies have shown that inflammation events can take place after the initial sequestration step. This means that membrane unfolding is probable for leukocytes after initial sequestration and development of local inflammation. A full understanding of the biochemical and mechanical events that occur during sequestration has not yet emerged and, in this context, membrane unfolding can be of great interest in leukocyte-endothelial cells interactions by mediating/aggravating the inflammatory processes.

Actin and actomyosin activity do not drive the cell shape recovery

When a leukocyte is expelled from a narrow capillary into a larger channel, it recovers its spherical shape in two stages. The first stage is fast and leukocytes almost recover their initial spherical shape in a characteristic time of 50 seconds, which is in very good agreement with previous observations (Tran-Son-Tay et al., 1991). A remarkable result is that the shape recovery process was found to be unaffected by perturbations of actin organization or actomyosin activity. Normal and treated THP-1 cells undergo a similar shape recovery. Moreover, this shape recovery was also found to be independent of the duration of sequestration in the narrow capillary. These results raise the question of the origin of the driving force leading to the shape relaxation, since it cannot be ascribed to actin polymerization nor to actomyosin activity. On the other hand, it is interesting to recall that velocity measurements have previously shown that the viscoelastic properties of normal, Jpk- and LatA-treated cells were still very different after the forced passage in the constriction. One can then conclude that the mechanism driving cell shape relaxation is robust enough to dominate the effect of different viscoelastic properties of cells with different actin cytosekeleton organizations. A mechanism that drives the global cell shape and applies forces on a several micron scale requires the (re)-building of a large macromolecular scaffold. The three major filamentous constituents of the cytoskeleton are potentially involved in the constitution of this scaffold. Our results obtained with Jpk- and LatA- treated THP-1 cells provide the first piece of evidence that actin is not dominantly involved in cell shape relaxation. Others have already presented results suggesting that microtubules play a negligible role in the mechanical properties of circulating leukocytes (Chien et al., 1984; Hofman et al. 1999; Saito et al. 2002; Tsai et al., 1996). This leaves intermediate filaments as the most probable actor in cell shape recovery after deformation. It is quite interesting to remark that this conclusion is consistent with recent experiments on lymphocytes (Brown et al., 2001), which demonstrate that vimentin intermediate filaments are the main contributors to the stiffness of circulating lymphocytes. For the future, our results strongly suggest that it would be very interesting to further investigate the specific and precise role of intermediate filaments in the different stages of leukocytes trafficking through narrow capillaries.

A deformed leukocyte state is required for normal trafficking through the capillary bed

The kinetics of cell relaxation helps to shed light on the behavior of leukocytes in physiological conditions where they have to negotiate the passage through not only one but several connected constriction segments from an arteriole to a venule. The number of segments encountered during the human pulmonary transit is estimated from 50 to 100 (Hogg and Doerschuk, 1995) and the transit time of individual canine leukocytes was measured in vivo at a median value of 26 seconds with very large deviations (Lien et al., 1987). The characteristic recovery time of 50 seconds observed in our microfluidic experiments for restoring the main part of the leukocyte spherical shape after deformation is therefore of particular interest. Indeed, the recovery rate of deformed leukocyte is not fast enough to allow a complete shape recovery in physiological transit conditions. This suggests that deformed leukocyte shapes may facilitate their transit through subsequent restrictions imposed by the capillary bed (Gebb et al., 1995). The versatility of the microfluidic technique allowed us to confirm this assumption with a special design mimicking the geometry of physiological segments.

Conclusions

We have used a microfluidic technique to investigate the passage of leukocytes in a narrow capillary, which is the starting event of post-sepsis or trauma disorders in the lung microvasculature. This in-vitro and single-cell approach provides an improved understanding of the role of actin and myosin II on capillary leukocyte trafficking in physiologically relevant mechanical and hydrodynamical conditions. We have established that the redistribution of actin filaments and molecular motor activity have specific and different roles on the extent and rate of cell deformation and cell membrane unfolding in the different stages of leukocyte trafficking in a constriction (entry stage, transit stage and shape recovery stage). Leukocyte entry times into a capillary and hydrodynamic friction with the capillary walls are strongly enhanced by the degree of actin polymerization. This confirms the important role of the actin network organization for the sequestration of leukocytes in capillaries. Our results also provide the first assessment of the contribution of myosin II activity to cellular transit in narrow capillaries. Myosin II activity influences only marginally the global cell mechanical properties but appears as a

key element in the mechanism of membrane unfolding under stress. Finally, the cell shape recovery time of 50 seconds was shown to help significantly the transit through the capillary segment network. Importantly, we also showed that the characteristic time of cell shape recovery is not driven by actin polymerization nor actomyosin activity, which suggests that the role of intermediate filaments should be systematically investigated in each stage of traffic through a capillary.

Materials and Methods

Cell preparation and drug treatments

We used the monocytic THP-1 line (Tsuchiya et al., 1980) maintained as previously described (Vitte et al., 2004) in Roswell Park Memorial Institute-1640 medium (Invitrogen, Cergy Pontoise, France) supplemented with 20 mM HEPES buffer, 10% Fetal Calf Serum (FCS), 2mM L-Glutamine, 50 U/ml penicillin and 50 µg/ml streptomycin. Stock cell culture were passaged twice weekly and maintained at 37°C in a humidified atmosphere containing 5% CO_2. Jasplakinolide (Molecular probes, J7473, Eugene, OR) 1.4 mM, Latrunculin A (Molecular Probes, L12370, Eugene, OR) 2.37 mM and Blebbistatin (Fischer Bioblock Scientific, Illkirch, France) 75 mM stock solutions were prepared in dimethyl sulfoxyde (DMSO) and stored at -20°C. Cells ($1x10^6$/mL) were incubated with Jpk, LatA and Blebbistatin at concentrations of 3, 3 and 50 µg/ml respectively on a rocking platform for 20 minutes at 37°C. Control experiments have ensured that DMSO up to 0,5% does not affect THP-1 mechanical properties.

Microfluidic setup

Microfluidic channels are first drawn using Clewin software (WieWeb Software, Netherlands) and a chromium mask is generated (Toppan Photomask, Corbeil Essonnes, France). A master of the channels was then fabricated on a silicon wafer by photolithography with photosensitive resins (SU-8 2015, Microchem, MA, USA). Microfluidic channels were molded with polydimethylsiloxane (PDMS, Sylgard 184 Silicone Elastomer Kit, Dow Corning, USA). Ports to plug the inlet and outlet reservoirs were punched in the PDMS replica with a gauge needle. The device is finalized by sealing the PDMS piece on a 170 µm thick glass coverslips via O_2-plasma activation of both surfaces. Inlet and outlet reservoirs are connected to the microfluidic device with Teflon tubings and the reservoirs are attached to a linear translation stage mounted on a linear slide. Pressure drops across the microchannel are controlled by varying the height between inlet and outlet macroreservoirs (Fig. 1).

Microfluidic design rationale

A spherical cell of diameter D_i squeezed in a slit of width W is deformed into a puck of height W and diameter D_{pu}. Considering that the free edge of the squeezed puck has a curvature imposed by W, the apparent D_{pu} can be calculated as:

$$D_{pu} = W(1-\frac{\pi}{2}) + \sqrt{(\pi W)^2 + \left(\frac{8D_i^3}{3W}\right)}$$

For D_i = 12.5 µm and W = 4 µm, the deformed puck-shaped cell has a diameter D_{pu} = 16.8 µm. Therefore, the height H of our microfluidics channels was chosen at 16 µm. This value permits a free travel of cells of diameter D_i = 12.5 µm in the inlet and relaxation channels of cross-section 20x16 µm, and insure also that the deformed cells fill the constriction cross section of 4 x 16 µm. Therefore, the pressure drop across the constriction applies fully on the cells with minimum fluid leakage around it. On the other hand, the microfluidics experiments were also designed regarding the forces exerted on a cell in the constriction. The force F_p, exerted by the pressure drop ΔP and pushing the cell along the channel is:

$$F_p = WH\Delta P$$

The friction force F_f, exerted by the lubrication liquid film separating the cells from the walls and opposing to the cell movement is:

$$F_f = \frac{\pi D_{pu}^2 \eta v}{2\delta}$$

where η is the viscosity of the medium, v is the velocity of the cell and δ is the thickness of the thin liquid film between the cell and the walls. Taking typical values of ΔP= 200 Pa, v = 2 10^{-4} m.s^{-1}, and δ = 100 nm (Bathe et al., 2002) leads to a ratio $F_f/F_p \approx 1.1$. F_f and F_p are of the same order of magnitude, so that friction changes will induce detectable velocity changes in the constriction.

Microfluidic experiment of cell passage through a constriction.

Microfluidic devices were first incubated with 1% pluronic F108 solution (BASF, NJ) for 2 h to deter cell adhesion (Jo and Park, 2000). A Nikon incubator NP-2 was used to control the temperature at 37°C. HEPES (N-2-hydroxyethylpiperazine-N'-2-ethanesulfonic acid) buffer (Sigma, MO, USA) was used to provide buffering of the media in the pH range (7.2-7.4 at 37°C). Before each experiment, THP-1 cells were centrifugated at 1750 rpm for 4 minutes (Eppendorf, model Centrifuge 5804R) and diluted in serum-free medium to 10^3 cells/mL before injection in the device with a syringe connected to the inlet. In some cases, cells formed small protusions and/or large pseudopods while in the microchannel or during shape recovery phase. These cells were excluded from this study. Cell viability was confirmed by the trypan blue exclusion test. All movies were taken using an Olympus inverted optical microscope (Olympus IX71) equipped with oil immersion objective lenses of magnification x60 (Olympus, PlanApo 1.40) and x100 (Olympus, UplanFLN 1.30), a CCD video camera (COHUE, model 4912-5000), a professional videotape recorder (Sony, model DSR-25). They were digitized and finally analyzed frame by frame with ImageJ software (Abramoff, 2004).

The authors gratefully acknowledge the Laboratoire du Futur of Rhodia (LOF, Pessac, France) for technical support with microfabrication and Rhodia Company for financial support of the SG's CNRS postdoctoral position. SG is now Chargé de Recherches of the F.R.S.-FNRS.

References

Abramoff, M. D., Magelhaes, P. J. and Ram, S. J. (2004). Image Processing with ImageJ**.** *Biophotonics Int.* **11**, 36-42.
Bathe, M., Shirai, A., Doerschuk, C. M. and Kamm, R. D. (2002). Neutrophil transit times through pulmonary capillaries : the effects of capillary geometry and fMLP-stimulation. *Biophys. J.* **83**, 1917-1933.
Bico, J. and Quéré, D. (2002). Self-propelling slugs. *J. Fluid Mech.* **467**, 101-127.
Bessis, M. (1973). Living blood cells and their ultrastructure. Springer, Berlin.
Bornens, M., Paintrand, M. and Celati, C. (1989). The cortical microfilament system of lymphoblasts displays a periodic oscillatory activity in the absence of microtubules: implications for cell polarity. *J. Cell Biol.* **109**, 1071-1083.
Brown, M. J., Hallam, J. A., Colucci-Guyon, E. and Shaw, S. (2001). Rigidity of circulating lymphocytes is primarily conferred by vimentin intermediate filaments. *J. Immunol.* **166**, 6640–6646.

Bubb, M. R., Senderowicz, A. M., Sausville, E. A., Duncan, K. L. and Korn, E. D. (1994). Jasplakinolide, a cytotoxic natural product, induces actin polymerization and competitively inhibits the binding of phalloidin to F-actin. *J. Biol. Chem.* **269**, 14869-14871.
Charras, G. and Paluch, E. (2008). Blebs lead the way : how to migrate without lamellipodia. *Nat. Rev. Mol. Cell Biol.* **9**, 730-736.
Chaw, K. C., Manimaran, M., Tay, F. E. H. and Swaminathan, S. (2006). A quantitative observation and imaging of single tumor cell migration and deformation using a muti-gap microfluidic device representing the blood vessel. *Microvascular Research*. **72**, 153-160.
Chien, S. and Sung, K. L. (1984). Effect of colchicine on viscoelastic properties of neutrophils. *Biophys. J.* **46**, 383-386.
Chien, S., Sung, K. L., Schmid-Schonbein, G. W., Skalak, R., Schmalzer, E. A. and Usami, S. (1987). Rheology of leukocytes. *Ann. N. Y. Acad. Sci.*, **516**, 333–347.
Damiano, E.R. (1998). The effect of the endothelial-cell glycocalyx on the motion of red blood cells through capillaries. *Microvascular Research*. **55**, 77-91.
Dewitt, S. and Halett M. (2007). Leukocyte membrane "expansion": a central mechanism for leukocyte extravasation. *J. of Leukocyte Biol.* **81**, 1160-1164.
Doerschuk, C. M., Beyers, N., Coxson, H. O., Wiggs, B. and Hogg, J. C. (1993). Comparison of neutrophil and capillary diameters and their relation to neutrophil sequestration in the lung. *J. Appl. Physiol.* **74**, 3040-3045.
Doerschuk, C. M. (2001). Mechanisms of leukocyte sequestration in inflamed lungs. *Microcirculation*. **8**, 71-88.
Downey, G. P. and Worthen, G. S. (1988). Neutrophil retention within model capillairies : role of the cell deformability, geometry and hydrodynamic forces. *J. Appl. Physiol.* **65**, 1861-1871.
Drury, J. L. and Dembo, M. (1999). Hydrodynamics of micropipette aspiration. *Biophys. J.* **76**, 110-128.
Evans, E., Leung, A. and Zhelev, D. (1993). Synchrony of cell spreading and contraction force as phagocytes engulf large pathogens. *J. Cell Biol.* **122**,1295-1300.
Franck, R. S. (1990). Time-Dependent Alterations in the Deformability of Human Neutrophils in Response to Chemotactic Activation. *Blood*. **76,** 2606-2612.
Frutos-Vivar, F., Nin, N. and Esteban, A. (2004). Epidemiology of acute lung injury and acute respiratory distress syndrome. *Curr. Opin. Crit. Care*. **10**, 1-6.
Fukuda, S. and Schmid-Schönbein, G. W. (2002). Centrifugation attenuates the fluid shear response of circulating leukocytes. *J. Leukoc. Biol.* **72**, 133-139.
Gebb, S. A., Graham, J. A., Hanger, C. C., Godbey, P. S., Capen, R. L., Doerchuk, M. and Wagner, W. W. (1995). Sites of leukocyte sequestration in the pulmonary microcirculation. *J. Appl. Physiol.* **79**, 493-497.
Hansell, P., Borgstrom, P. and Arfors, K. E. (1993). Pressure-related capillary leukostasis following ischemia-reperfusion and hemorrhagic shock. *Am. J. Physiol.* **265**, H381–8.
Herant, M., Heinrich, V. and Dembo, M. (2005). Mechanics of neutrophil phagocytosis : behavior of the cortical tension. *J. Cell. Sci.* **118**, 1789-1797.
Herant, M., Marganski, W. A. and Dembo, M. (2003). The mechanics of neutrophils: synthetic modeling of three experiments. *Biophys. J.* **84**, 3389-3413.
Hochmuth, R.M. and Needham, D. (1990). The viscosity of neutrophils and their transit times through small pores. *Biorheology*. **27**, 817-828.
Hofman, P., d'Andrea, L., Guzman, E., Selva, E., Le Negrate, G., Farahi Far, D., Lemichez, E., Boquet, P., Rossi, B. (1999). Neutrophil F-actin and myosin but not microtubules functionally regulate transepithelial migration induced by interleukin 8 across a cultured intestinal epithelial monolayer. *European Cytokine Network*. **10**, 227-36.
Hogg, J. C., McLean, T., Martin, B. A. and Wiggs, B. R. (1988). Erythrocyte transit and neutrophil concentration in the dog lung,. *J. Appl. Physiol.* **65**, 1217-1225.
Hogg, J. C., Coxson, H. O., Brumwell, M.-L., Beyers, N., Doerschuk, C. M., MacNee, W. and Wiggs, B. R. (1994). Erythrocyte and polymorphonuclear cell transit time and concentration in human pulmonary capillaries. *J. Appl. Physiol.* **77**, 1795-1800.
Hogg, J. C. and Doerschuk, C. M. (1995). Leukocyte traffic in the lungs. *Ann. Rev. Physiol.* **57**, 97–114.
Huang, Y., Doerschuk, C. M. and Kamm, R. D. (2001). Computational modeling of RBC and neutrophils transit through the pulmonary capillary. *J. Appl. Physiol.* **90**, 545-64.
Jay, P. Y., Pham, P. A., Wong, S. A. and Elson, E. L. (1995). A mechanical function of myosin II in cell motility. *J. Cell Sci.* **108**, 387-393.
Jo, S. and Park, K. (2000). Surface modification using silanated poly(ethylene glycol)s. *Biomaterials*. **21**, 605– 616.
Kansas, G. S. (1996). Selectins and their ligands: current concepts and controversies. *Blood.* **88**, 3259–3287.
Lämmerman, T., Bader, B. L., Monkley, S. J., Worbs, T., Wedlich-Söldner, R., Hirsch, K., Keller, M., Forster, R., Critchley, D. R., Fassler, R et al. (2008). Rapid leukocyte migration by integrin-independent flowing and squeezing. *Nature*. **453**, 51-55.
Lien, D. C., Wagner Jr., W. W., Capen, R. L. , Haslett, C. , Hanson, W. L., Hofmeister, S. E., Henson P. M. and Worthen, G. S. (1987). Physiologic neutrophil sequestration in the canine pulmonary circulation. *J. Appl. Physiol.* **62**, 1236-1243
MacCallum N. S. and Evans T. W. (2005). Epidemiology of acute lung injury, *Curr. Opin. Crit. Care* **11**, 43–49.
Martens, J. C. and Radmacher, M. (2008). Softening of the actin cytoskeleton by inhibition of myosin II. *Pflugers Arch - Eur. J. Physiol.* **456**, 95-100.
Nishino, N., Tanaka, H., Ogura, H., Inoue, Y., Koh, T., Fujita, K. and Sugimoto, H. (2005). Serial changes in leukocytes deformability and whole blood rheology in patients with sepsis or trauma. *The journal of Trauma*. **59**, 1425-1431.
Pai, A., Sundd, P. and Tees, D. F. J. (2008). In situ microrheologial determination of neutrophil stiffening following adhesion in a model capillary. *Ann. Biomed. Eng*. **36**, 596-603.
Petersen, N. O., McConnaughey, W. B. and Elson, E. L. (1982). Dependence of locally measured cellular deformability on position on the cell, temperature and Cytochalasin B. *Proc. Nat. Acad. Sci. USA*. **79**, 5327-5331.
Raucher, D. and Sheetz, M. P. (1999). Characteristics of a membrane reservoir buffering membrane tension. *Biophys. J.* **77**, 1992–2002.
Richelme, F., Benoliel, A.-M. and Bongrand, P. (2000). Dynamic study of cell mechanical and structural responses to rapid changes of calcium level. *Cell Motil. Cytoskeleton*. **45**, 95-113.
Rotsch, C. and Radmacher, M. (2000). Drug-Induced Changes of Cytoskeletal Structure and Mechanics in Fibroblasts - An Atomic Force Microscopy Study. *Biophys. J.* **78**, 520-535 .
Saito, H., Lai, J., Rogers, R. and Doerschuk, C. M. (2002). Mechanical properties of rat bone marrow and circulating neutrophils and their responses to inflammatorry mediators. *Blood*. **99**, 2207-2213.
Schmid-Schönbein, G. W., Shih, Y. Y. and Chien, S. (1980). Morphometry of Human Leukocytes. *Blood.* **56,** 866-875
Schmid-Schönbein, G. W. (1987). Capillary plugging by granulocytes and the no-reflow phenomenon in the microcirculation. *Fed. Proc.* **46,** 2397-2401.
Sheetz, M. P., Block, S. M. and Spudich, J. A. (1986). Myosin movement in vitro: a quantitative assay using oriented actin cables from Nitella. *Methods Enzymol.***134**, 531-544**.**
Sheetz, M. P. (1998). Laser Tweezers in Cell Biology**,** *Academic Press*, London, UK.
Sheikh, S., Gratzer, W. B., Pinder, J. C. and Nash, B. (1997). Actin polymerization regulates integrin-mediated adhesion as well as rigidity of neutrophils. *Biochem. Biophys. Res. Commun.* **238**, 910-915.
Simon, S. I. and Schmid-Schönbein, G. W. (1988). Biophysical aspects of microsphere engulfment by human neutrophils. *Biophys. J.* **53**, 163-173.
Skoutelis, A. T., Kaleridis, V., Athanassiou, G. M., Kokkinis, K. I., Missirlis Y. F. and Bassaris, H. P. (2000). Neutrophil deformability in patients with sepsis, septic shock, and adult respiratory distress syndrome. *Crit. Care Med.* **28**, 2355-2359.
Straight, A. F., Cheung, A., Limouze, J., Chen, I., Westwood, N. J., Sellers, J. R. and Mitchinson, T. J. (2003). Dissecting temporal and spatial control of cytokinesis with a myosin II inhibitor. *Science*. **299**, 1743-1747.
Sung, K. L. P., Dong, C., Schmid-Schönbein, G. W., Chien, S. and Skalak, R. (1988). Leukocyte relaxation properties. *Biophys. J.* **54**, 331–336.
Tabeling, P. (2005). Introduction to microfluidics, *Oxford University Press*, London, UK.
Thiel, M., Zourelidis, C. and Peter, K. (1996). The role of polymorphonuclear leukocytes in the pathogenesis of the adult respiratory distress syndrome. *Anaesthesist.* **45**, 113-130.
Thoumine, O. and Ott, J. (1997). Time scale dependent viscoelastic and contractile regimes in fibroblasts probed by microplate manipulation. *J. Cell Sci*., **110**, 2109-2116.
Tran-Son-Tay, R., Needham, D., Yeung, A. and Hochmuth, R. M. (1991). Time-dependent recovery of passive neutrophils after large deformation,. *Biophys. J.* **60**, 856-866.
Tsai, M. A., Waugh, R. E. and Keng, P. C. (1996). Cell cycle-dependence of HL-60 cell deformability. *Biophys. J.* **70**, 2023-2029.
Tsai, M. A., Waugh, R. E. and Keng, P. C. (1998). Passive Mechanical Behavior of Human Neutrophils: Effects of Colchicine and Paclitaxel. *Biophys. J.*, **74**, 3282–3291.
Tsuchiya, S., Yamabe, M., Yamaguchi, Y., Kobayashi, Y., Konno, T. and Tada, K. (1980). Establishment and characterization of a human acute monocytic leukemia cell line (THP-1). *Int. J. Cancer*. **26**, 171-176.
Vink, H. and Duling, B.R. (1996). Indentification of distinct luminal domains for macromolecules, erythrocytes, and leukocytes within mammalian capillaries, *Circ Res*. **79**, 581-589.

Vitte, J., Benoliel, A.-M., Eymeric, P., Bongrand, P. and Pierres, A. (2004). Beta 1 integrin-mediated adhesion may be initiated by multiple incomplete bonds, thus accounting for the functional importance of receptor clustering. *Biophys. J.* **86**, 4059–4074.
Wang, Q., Chiang, E. T., Lim, M., Lai, J., Rogers, R., Janmey, P. A., Shepro, D. and Doerschuk, C. M. (2001). Changes in the biomechanical properties of neutrophils ans endothelial cells during adhesion. *Blood*. **97**, 660-668.
Wakatsuki, T., Wysolmerski, R. B., and Elson, E. L. (2003). Mechanics of cell spreading : role of myosin II. *J. Cell Sci.*, **116**, 1617-1625.
Weibel, E. R. (1963). Morphometry of the Human Lung (New York: Academic Press Inc).
West, J. B. and Mathieu-Costello, O. (1995). Vulnerability of Pulmonary Capillaries in Heart Disease. *Circulation*. **92**, 622-631.
Wong, P. K., Tan, W. and Ho, C. -M. (2005). Cell relaxation after electrodeformation : effect of latrunculin A on cytoskeletal actin. *J. Biomech*. **38**, 529-535.
Worthen G. S., Schwab B., Elson E. L. and Downey G. P. (1989). Mechanism of simulated neutrophils : cell stiffening induces retention in capillaries. *Science*. **245**, 183-186.
Yap, B. and Kamm, R. D. (2005). Mechanical deformation of neutrophils into narrow channels induces pseudopods projection and changes in biomechanical properties. *J. Appl. Physiol.* **98**, 1930-1939.
Yoshida, K., Kondo, R., Wang, Q. and Doerschuk, C. M. (2006). Neutrophil Cytoskeletal Rearrangements during Capillary Sequestration in Bacterial Pneumonia in Rats. *Am. J. Respir. Crit. Care Med.* **174**, 689-698.

Figures

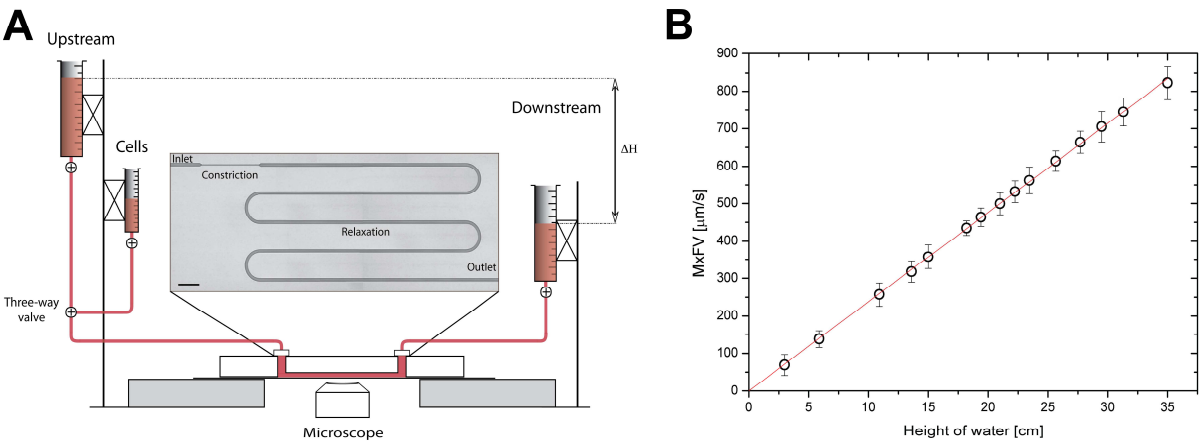

Fig. 1. Microfluidic setup. (A) Pressure drops were imposed by varying the height of water, ΔH, between the upstream and downstream macroreservoirs. Cells were introduced into the device by a syringe connected to the upstream reservoir with a three-way valve. The inset shows a picture of the 4-µm-wide constriction channel (length : 2250 µm) and 20-µm-wide inlet/oulet channels. The scale bar corresponds to 850 µm. (B) Maximum fluid velocity measured by fluorescent particles tracking, MxFV, versus ΔH. Values are means ± SE; n = 4.

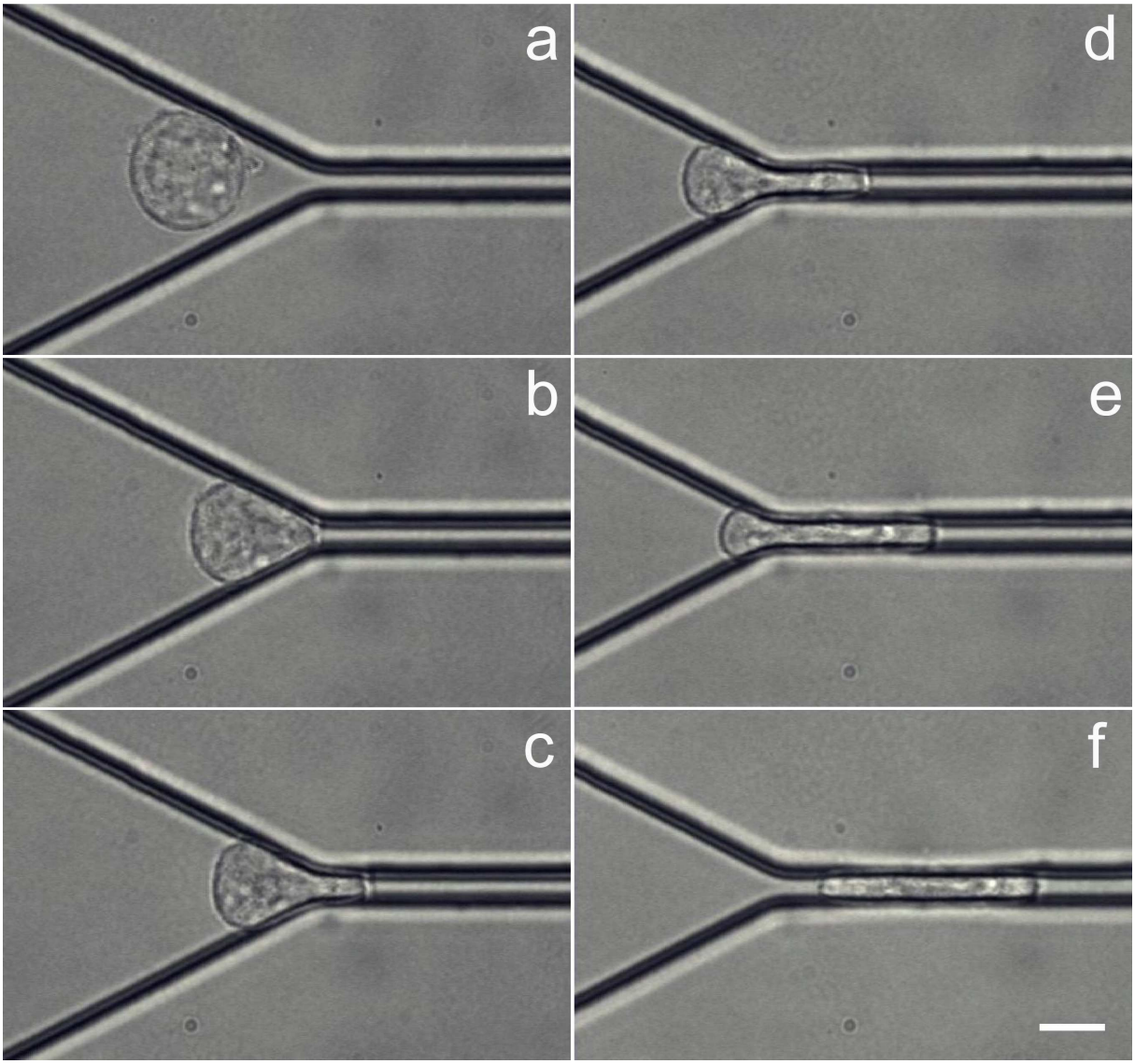

Fig. 2. Images sequence of a Blb-treated THP-1 cell during entry in the 4-µm-wide constriction (ΔH = 10,8 cm H_2O). (a) approach, (b) contact, (c), (d) and (e) development of a projection in the constriction, and (f) completed entry. The scale bar represents 12 µm.

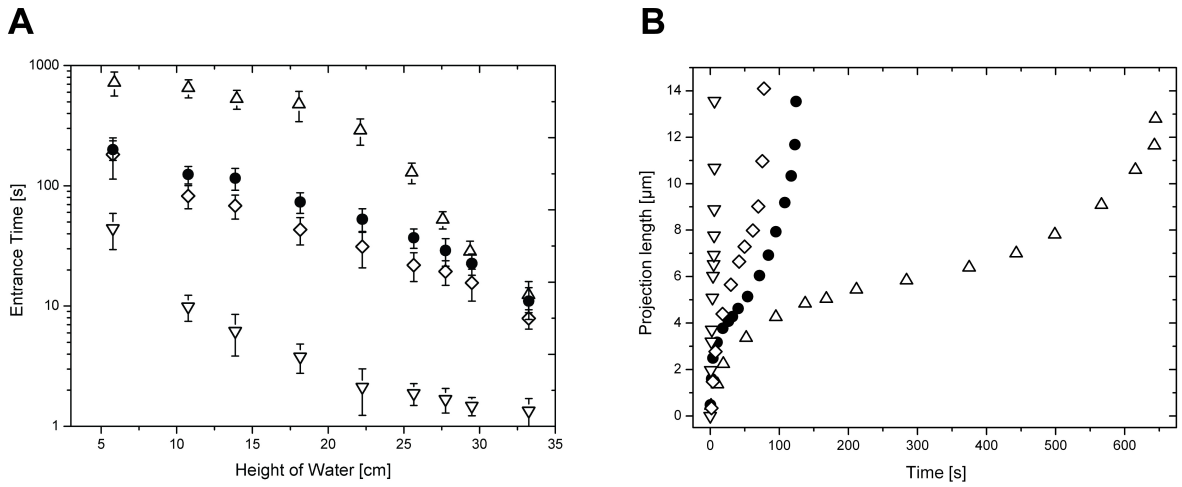

Fig. 3. Role of the actin cytoskeleton and actomyosin activity during entry stage. (A) Entry times, ETs, versus height of water, ΔH, and (B) projection length L_m versus time at ΔH = 10,8 cm H_2O in a 4-µm wide constriction for normal (●), Blb-treated (◇), Jpk-treated (△) and LatA-treated (▽) THP-1 cells. Error bars represent standard error (THP-1 : n=7, LatA : n=4, Jpk : n=4, Blb : n=6).

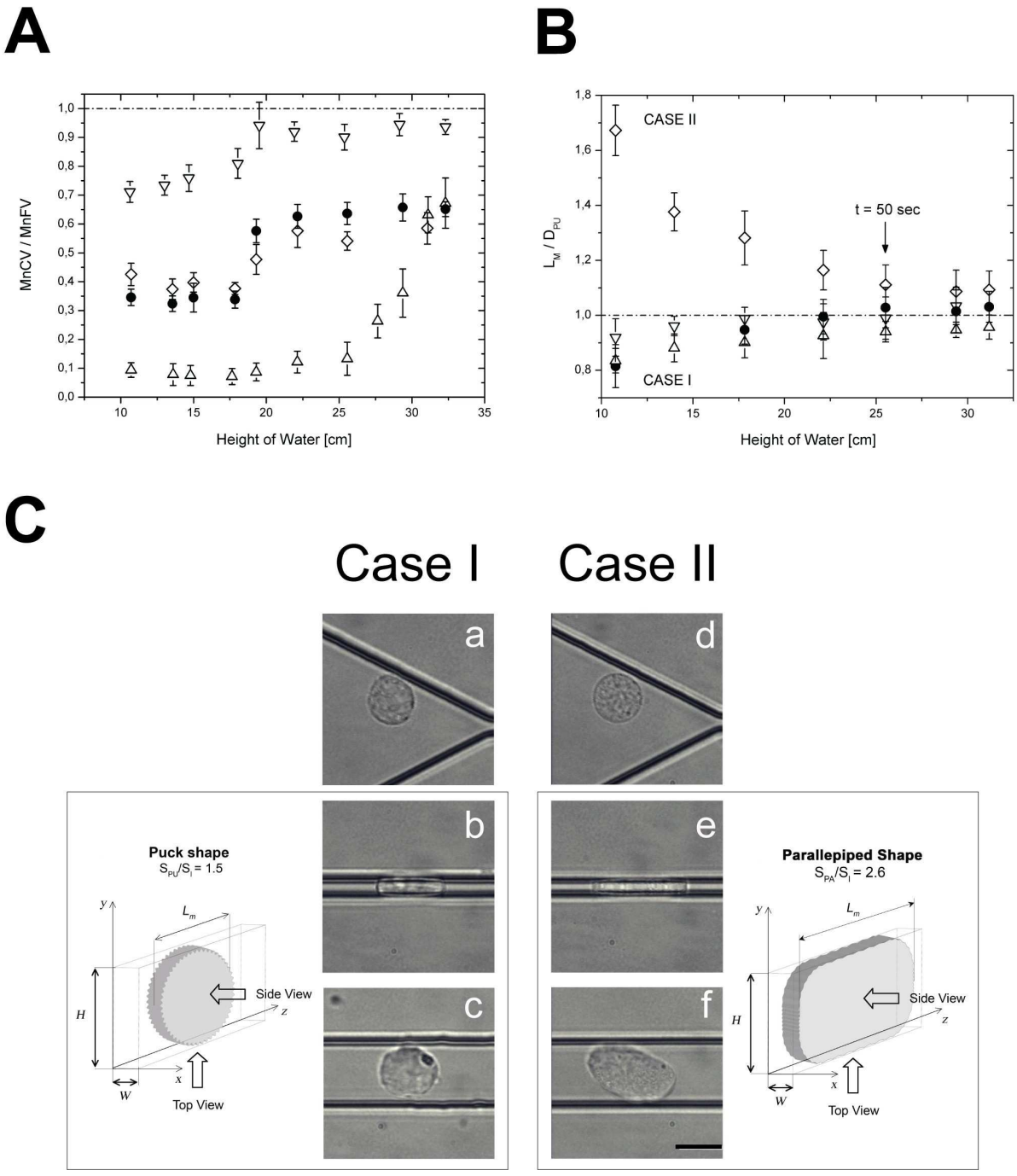

Fig. 4. Role of the actin cytoskeleton and actomyosin activity during transit stage. (A) Ratio mean cell velocity/mean fluid velocity, MnCV/MnFV, and (B) ratio projection length/puck diameter, L_m/D_{pu}, as a function of the height of water, ΔH, for normal (●), Blb-treated (◇), Jpk-treated (△) and LatA-treated (▽) THP-1 cells. (C) Microscope pictures of THP-1 cells before entry in the constriction [a], in the constriction [b], and shortly after their release from the constriction when the free-rotating cell presented a maximum size [c]. Pictures [b] and [c] give respectively insight into the top- and side-views of the cell in the constriction. Case I: Control, Jpk-treated and Lat-A-treated cells have a puck shape with diameter 17 μm , height W= 4 μm and excess surface area ΔS/S=50% (left cartoon). Case II: Blb-treated cells have a roughly parallelepipedic shape with dimensions 4, 16 and 29 μm and excess surface area ΔS/S=160% (right cartoon).

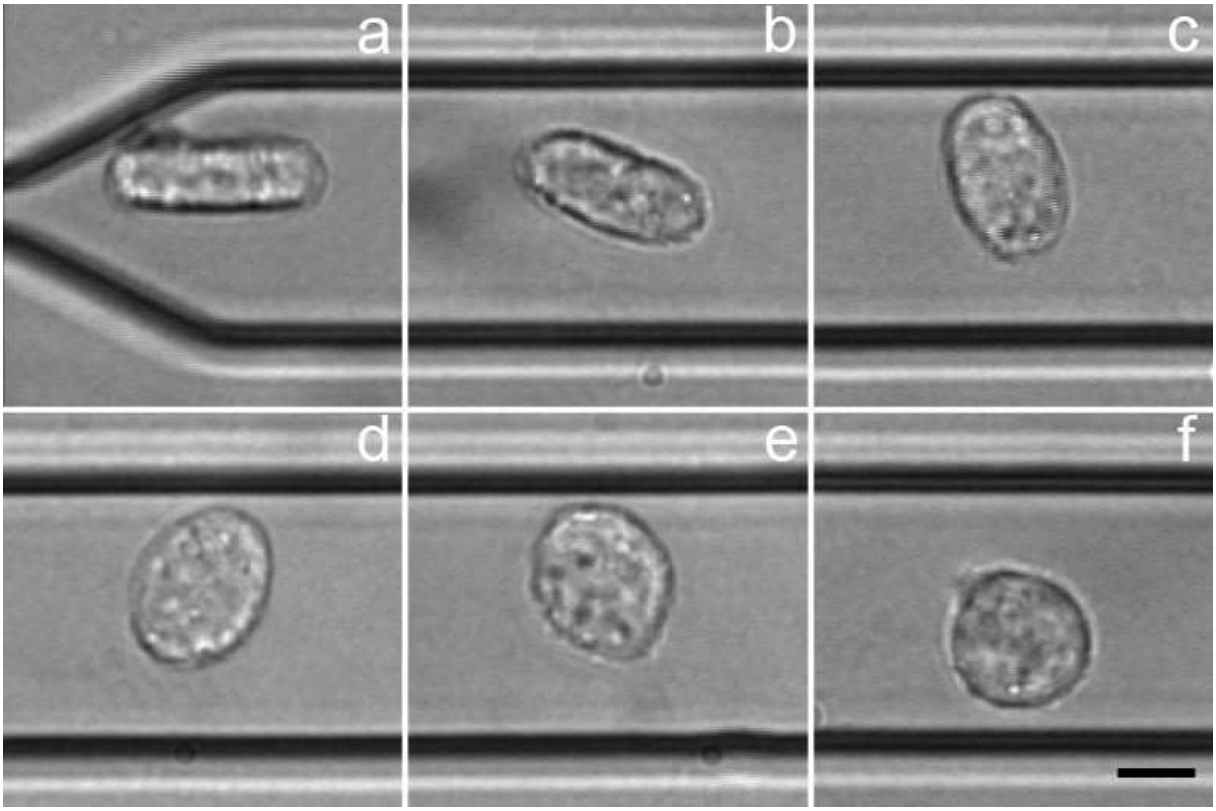

Fig. 5. Image sequence a THP-1 cell at different times after release from a 4-µm-wide constriction (a) t = 0,6 s, (b) t = 7,2 s, (c) t = 26 s, (d) t = 41,7 s, (e) t = 204,3 s and (f) t = 413,5 s. The scale bar represents 8 µm.

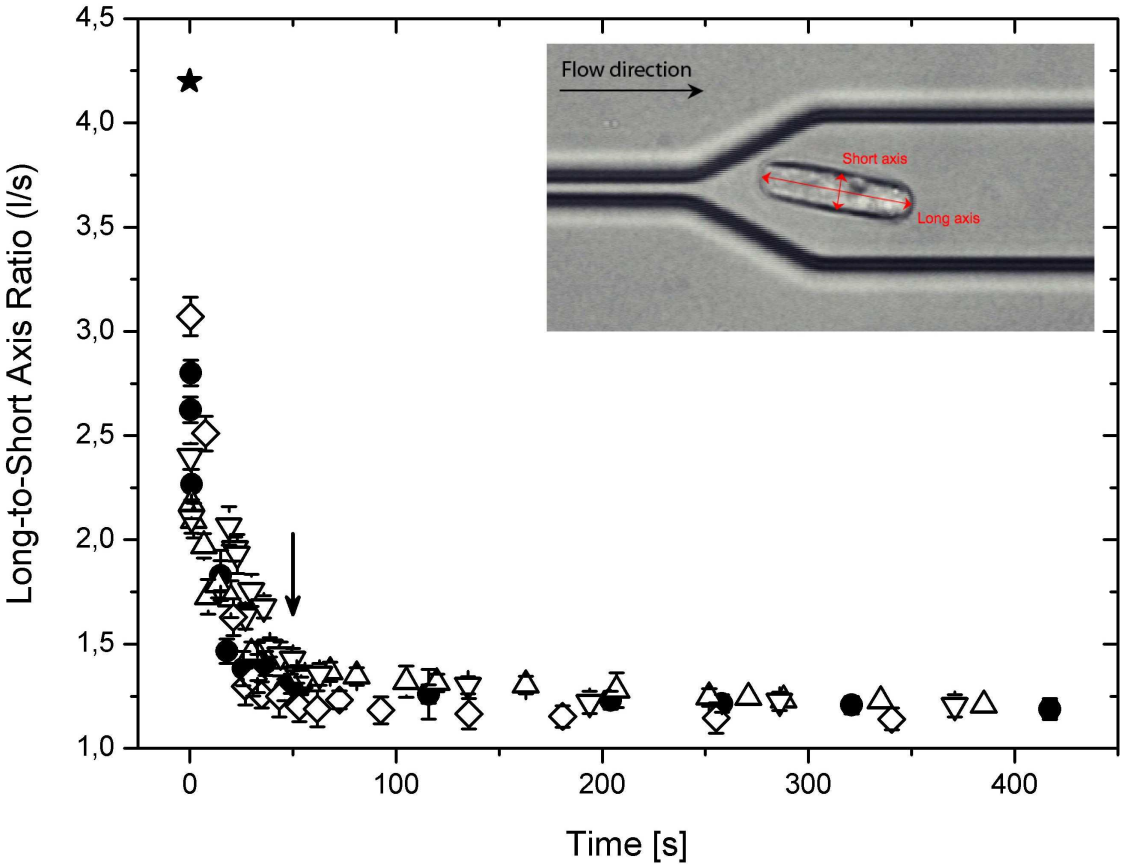

Fig. 6. Role of the actin cytoskeleton and actomyosin activity during relaxation stage. Long-to-short axis ratio (l/s) of a THP-1 cell versus the time after release from a 4-µm-wide constriction. Error bars represent standard error (THP-1 (●): n=4, LatA (▽): n=3, Jpk (△): n=4, Blb (◇): n=3). The ★ sign at t=0 corresponds to the theoretical l/s ratio of a puck with diameter 16.8 µm and height W= 4 µm. The inset shows long (l) and short (s) axis on a picture of a deformed cell.

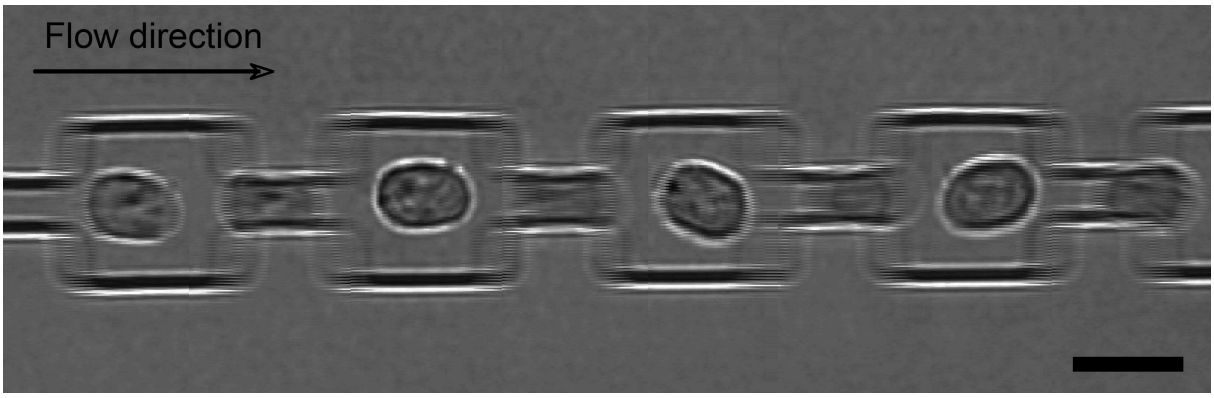

Fig. 7. Series of images showing the passage of a single THP-1 cell through a succession of 5-µm-wide segments. The scale bar represents 15 µm.

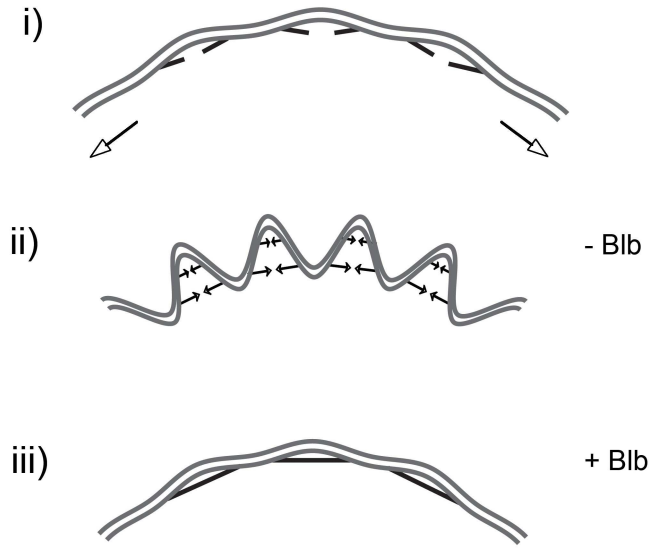

Fig. 8. Scheme of the actomyosin activity contribution to membrane folding. (i) Cell membrane after a large expansion. Microvilli are unfolded and membrane-cytoskeleton-membrane links are cleaved. (ii) Normal cells: links rebuild and myosin II exerts tension (arrows) to re-wrinkle the membrane. (iii) Blb-treated cells: without myosin II tensile activity links may reform but membrane is not wrinkled after 50 seconds.

Supplementary materials

Movie 1. Sequence of a Lat-treated THP-1 cell of diameter D_i = 12 μm circulating successively in the inlet channel (cross-section 20x16 μm), the constriction channel (cross-section 4x16 μm) and the relaxation channel (cross-section 20x16 μm) at an applied driving pressure of 13 cm H_2O. The visualization of the entry, transit and relaxation stages permits to investigate the deformation kinetics during entry in the constriction, the cell velocity during capillary transit, and the shape recovery kinetics after release from the constriction.

Movie 2. Sequence of a normal THP-1 cell of initial diameter D_i = 12.5 μm released from the constriction channel at an applied driving pressure ΔH of 18 cm H_2O. The free rotation of the cell in the relaxation channel allows access to a side-view of the deformed cell approximately 1 second after its release from the constriction. The deformed shape in this case corresponds to the minimal deformation into a puck of height W ~ 4 μm and diameter D_{pu} ~ 16 μm.

Movie 3. Sequence of a normal THP-1 cell of initial diameter D_i = 12 μm circulating through a succession of 5-μm-wide and 20-μm distant segments at a driving pressure ΔH of 25 cm H_2O. The elongated shape adopted by circulating leukocytes helps their passage through successive segments.